STRUCTURAL DAMAGE IDENTIFICATION USING DYNAMIC NUMERICAL MODELS

A. Samartín, P. Tabuenca, J. García-Palacios
Escuela Técnica Superior de Ingenieros de Caminos, Canales y Puertos. UPM. Prof. Aranguren sn. 28040 Madrid, España. Escuela Superior de la Marina Civil. Plaza de Gamazo. UC. Santander, España
avelino@mecanica.upm.es, tabuencp@unican.es, jgpalacios@caminos.upm.es

1 Summary

In this paper a review of two main groups of structural damage identification methods by dynamic tests is presented. The first group is concerned with metallic thin structures damages or imperfections and the second one with reinforced concrete beam structures damages.

1. The first group is addressed to the detection of potential imperfections, fissures and cracks appearing in industrial machines, aeronautical structures and motor engines. They are typically metallic structures and the tests are carried under controlled environment conditions, such as in a laboratory. The application of body waves, and more often, guided waves, as Rayleigh and Lamb waves, as dynamic excitation in order to detect the damage, is described.

   The studied imperfections have been divided into three classes.

   - Cracks, related to the structural safety. They are penetrating a significant part of the plate thickness.
   - The second class of imperfections are small cracks or fissures, and they can be called partially penetrating ones because they are extended only to a small part of the plate thickness. Imperfections of this class are difficult to detect, because sometimes they can not be observed on the plate surfaces.
   - Finally, the third class of imperfections are the superficial cracks and they are more related to the durability of the structure than to its safety. These imperfections are more connected to structural protection to the environment, i.e. to protective painting and coating.

   Dynamic models used to detect the first class of imperfections have been Kirchhoff or Reissner bending thin plate. The crack detection can be achieved quite accurately by comparison between the first spatial derivatives of the mode shapes of the uncracked and cracked plates. Partially penetrating and superficial cracks have been identified by application as dynamic input of Lamb and Rayleigh waves respectively. The use of these guide waves seems to be a very promising technique for imperfection detection. However, computational problems appear. They are related to the small time step and the large number of the finite elements needed in order to reach a suitable accuracy level.

2. The second part of the paper treats a different group of dynamic identification and location of damage in civil and building structures. In particular the damage in reinforced concrete beams, typically used in bridge and building structures is studied. Detection procedures in this part differ of the first ones, because the existing structure is tested in the field and reinforced concrete is rather heterogenous material in comparison to metallic material. Normally, potential cracks are detected, during the free vibrations of the structure, by estimation of the changes either of its natural frequencies, or in its mode shapes or in the measure of its dynamic flexibility. However, in general, the differences of these values between uncracked and cracked beams are small and in some cases they can not be distinguished from the inherent measurement errors occurring during the tests.

   After reviewing several different models applied to crack detection, one based on the linear elasticity has been developed. In this model the cracks are assumed to remain open and the rest of the structure to behave elastically, Using this model a sensitivity analysis of the presence of cracks, depth and location, respect to the variation of the structure natural frequencies and modes shapes can be carried out. Using this approach a crack identification methodology is proposed. Finally, some possible modifications of the proposed methodology aimed to improve the accuracy and reliability of the obtained results are discussed.

Keywords

Damage detection, metallic plate structures, reinforced concrete structures, free vibration response, Rayleigh and Lamb waves, structural health monitoring

2 Introduction

Normally, in industrialized countries relatively few new public works (bridges, dams etc) are currently built and instead maintenance of already existing constructions is needed. Then, management of public structures is an important and rapidly demanding task to be carried out by Public Administration in these countries. This management includes maintenance and control about the structural performance of constructions. Typically the actual geometric and structural characteristics of these works are not known exactly, except if they are permanently monitored, and during their service life they can be deteriorated. Therefore, it is important to estimate their actual performance and level of safety. In this way different decisions respect to their eventual repairing or their use under extraordinary circumstances etc., can be taken.

In this direction several research programs in EU are currently under way to develop methodologies aimed to estimated the deterioration level, state and expected life of the existing structures. Among these research teams it can mentioned [BW96] and [PDPS95]. Most of the techniques used are directed to find tools, usually non destructive tests based on applying dynamic excitations to the structure [WHFY01], able to detect the existence of structural imperfections (crack, material deterioration etc.).

Two main groups of damage detection will be discussed in this paper. The first is concerned with structures composed by metallic plates and that can be tested under controlled environment conditions, usually in a laboratory. The technique used to identify different classes of damage varies according to the potential structural deterioration.

Three main types of imperfections in thin structures such as plates and shells will be studied:(1) body cracks or cracks that penetrate to the whole thickness of the structure, (2) superficial cracks that affect only to a very small part of the thickness and (3) partially penetrating cracks as an intermediate imperfection between the two former ones. The first type of imperfections is relevant to the structural safety and the second is more concerned with its maintenance and protection against environment attacks. The third type of imperfections appears very often in the damaged structures. In the study of the first type of imperfections the Kirchhoff theory of thin plates under dynamic loading will be applied. For the second type of imperfections superficial waves theory will be used. Among the superficial waves, Rayleigh waves, will be considered because the superficial cracks under investigation are assumed to penetrate a very small depth in comparison to the whole plate thickness. The partially penetrating cracks will be analyzed by means of Lamb waves.

The part of paper related with this type of damage detection corresponds to the first part of a joint research work named *Development of new techniques for non-contact, non-destructive testing by ultrasound* in which several Departments of the Technical University of Madrid and the University of Vigo are involved. In this research structural dynamic excitation devices and instruments for measurement of response are developed to detect possible imperfections in different structures, either in laboratory or in situ conditions. Here, only the part of this research related to theoretical aspects needed to mathematically simulate the behavior of structures under dynamic excitation is presented. With the help of these results it may be possible to identify the imperfection, i.e. its existence and also its position and geometry as well. This theoretical work will be divided into two phases. In the first phase the effects on the structural response of the presence of a imperfection (crack, changes of geometry or material properties, etc) is analyzed. The subsequent second phase is the inverse problem or identification problem i.e. to find the position and geometry of the imperfections from the knowledge of the response of a damaged structure. This phase will not be addressed here. It will be noticed in the next sections that some of the proposed techniques for damage detection avoid or at least simplify in many cases the application of methods to solve the inverse problem.

The second group of damages are related to bridges and building reinforced concrete structures. They are tested usually in the field under very noisy conditions (uncontrolled traffic, temperature etc.) and difficult access conditions. It is clear that, the methodology used for these cases has to be totally different to the previous one.

The importance of the detection of this group of damages is increasing during the last years. Health monitoring of existing civil and building structures is a very important topic of research. According to report published by USA Federal Highway Administration [Fed97] about a 42 % of highway bridges are deficient. Then, it becomes necessary to limit for them the collapse and service loading and also to

control their vulnerability to an increasing static and dynamic traffic and use loads. As a consequence, since some years damage assessment of structures has drawn the attention from different engineering areas. Static and dynamic non-destructive field tests have extensively been used as damage identification tools, although the dynamic identification methods have attracted more extensive research.
Different methods damage detection of reinforced concrete beams by dynamic tests are currently reported in the literature. In essence all these methods consist in the following steps. (1) obtain the dynamic response of the uncracked structure either in the design analysis step or by a dynamic test just after the structure completion, (2) dynamic test of the cracked structure, (3) select one or several dynamic system characteristics (DSCs), i.e. natural frequencies, modal shapes or dynamic flexibilities, for comparison between the responses of the cracked and the uncracked structures (4) develop an analytical model of the dynamic behavior of the cracked structure and (5) identify the positions and severities of the cracks from the differences between of DSCs previously obtained. This last step of identification it is also known as inverse problem for the crack model. To solve this problem it is necessary to solve a minimization problem, i.e. to find the positions and depth of the cracks such that the difference, according to some norm, between the observed dynamics DSCs for the crack and uncracked structures is minimum. Several optimization algorithms are available in order to solve the minimization problem, descendent gradient, penalization, genetic simulations, neural networks etc. in the specialized numerical literature.
A review of the current methods of structural damage detection is presented. The different DSCs used and the models aimed to simulate the free vibrations of the cracked reinforced concrete beam are emphasized. Among these different models, needed during the cracks identification step, special attention to the one presented in [CB84], that corresponds to a simplified cracked Navier-Bernoulli (N-B) beam elastic theory is discussed. An extension of this model, that includes the possibility to consider the existence of several non symmetric cracks, i.e. cracks appearing only in one of the two beam faces, is given. Therefore, it can be seen that the dynamic behavior of the cracked beam can be expressed by the behavior of a uncracked N-B beam of longitudinally variable cross section. The characteristics of this equivalent beam depend on the crack position and the crack depth. By application of the method of finite element (FE) the DSCs can be computed. Finally, using an identification procedure based on an error function between the computed and the experimental results it is possible to find the cracks positions and their severity.
The paper is organized as follows. In the first sections the three methods of damage detection of metallic structures based on body waves, Rayleigh waves and Lamb waves are reported. In the following sections a short revision of different approaches of damage detection of reinforced concrete beams is presented. Finally, in the framework of an elastic cracked N-B beam theory and based on the Hu-Washizu variational theorem a model is described and then applied to the damage detection. The paper concludes with a discussion about possible improvements to the model in order to increase the accuracy and reliability of its results.

3 Metallic plates. Penetrating cracks

As it has been shown in [SM02] the existence and position of cracks penetrating throughout the depth of a metallic plate can be obtained by low frequency dynamic tests with out-plane excitation, i.e. subjected to bending. The first derivatives, i. e. the rotations, of the shapes modes of the plate under free vibrations can be used to this end.
In order to illustrate this possibility a simple example will be considered. Let it be a square plate of side a, thin thickness h and simply supported along its perimeter. The dynamic behavior of this plate is described by the following initial value-boundary value problem:

$$\begin{aligned}
\nabla^4 w &= -\frac{\rho h}{D}\frac{\partial^2 w}{\partial t^2}, \quad \text{in} \quad 0 \le x \le a, \quad 0 \le and \le a \\
w = \frac{\partial^2 w}{\partial x^2} &= 0 \quad \text{along the boundaries and } \forall t \quad x = 0, x = a \\
w = \frac{\partial^2 w}{\partial y^2} &= 0 \quad \text{along the boundaries and } \forall t \quad y = 0, y = a \\
w &= f_0(x,y) \quad \text{at } t = 0 \\
\frac{\partial w}{\partial t} &= f_1(x,y) \quad \text{at } t = 0
\end{aligned} \tag{1}$$

in which $w = w(x, y, t)$ is the plate deflection orthogonal to its midplane, $f_0(x, y)$ and $f_1(x, y)$ two specified functions, ρ the mass per volume unit, E the Young modulus and ν the Poisson coefficient of

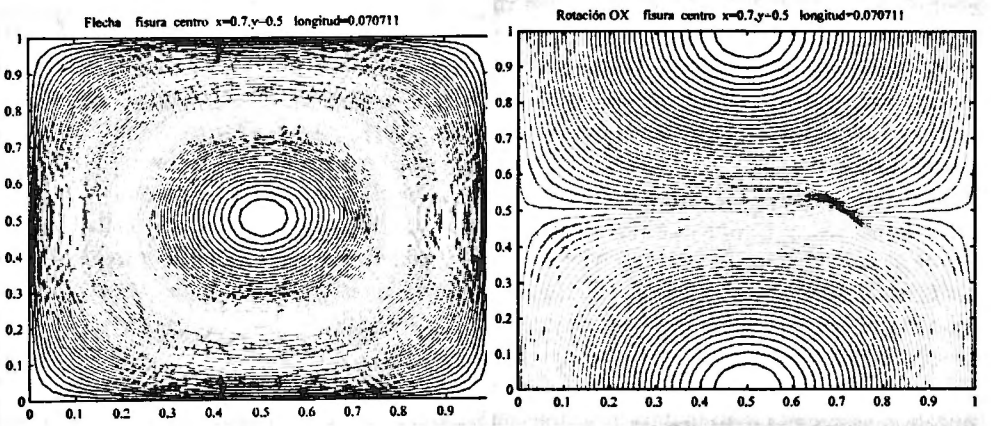

Figure 1: Modal vector 1. Plate with inclined crack at $(0.7a, 0.5a)$ and length $0.07a$. (a) Deflection w isolines (b) Rotation θ_x isolines

the plate material. The bending plate constant D is defined by the following expression:

$$D = \frac{Eh^3}{12(1-\nu^2)}$$

As it is very well known the natural frequencies ω_{mn} and the corresponding modes Φ_{mn} are:

$$\omega_{mn} = \pi^2 \sqrt{\frac{D}{\rho h}} \left[\left(\frac{m}{a}\right)^2 + \left(\frac{n}{a}\right)^2 \right]$$

$$\Phi_{mn} = w_{mn} \sin\left(\frac{n\pi x}{a}\right) \sin\left(\frac{n\pi y}{a}\right)$$

where w_{mn} is a normalizing constant.

This closed form solution has been compared to a numerical solution obtained by a Finite Element (FE) method in order to calibrate the FE mesh refinement necessary to obtain the results with a given degree of accuracy. Then, the plate has been modelled by square bending Tocher-Felippa elements. A FE mesh composed by 40×40 elements was used and the relative error obtained for the first natural frequency was $0,05\%$. Similar error orders have been reached in relation to the vibration modal vectors $\Phi_{mn} = (\Phi_{mn,i})$, using different comparison norms, such as, L_2, standard quadratic deviation, and L_∞ the difference between the maximum components of normalized modal vectors.

The next step was to assume the same plate with a totally penetrating crack throughout its thickness. The crack could be placed in any point of the plate and have arbitrary length. Then the plate was identified by the following parameters: the crack center x, y, its length l and inclination angle in plan or angle α respect the axis Ox. Using a similar FE mesh as before a sensitivity analysis was carried out, i.e. the natural frequencies and modes of the cracked plate were obtained. In each analysis the crack was defined by different set of parameters,x, y, l and α, that varies within a large range of values.

A conclusion derived from the former sensitivity analysis was the nonexistence of significative differences (less than 2 % using different norms) between the dynamic characteristics (first natural frequencies and modal vectors) of the non cracked and cracked plates. Therefore comparison between the first frequencies and modal vectors of damaged and undamaged plates may not lead to detection of a damage existence, although in case of comparison between high order natural modes discontinuities may be appeared in case of coincidence of the crack with the maximum or minimum of the vibration mode.

A more efficient way to detect damage consists in visualize the different isolines for the normal deflection w and rotations θ_x and θ_y of the plate. In case of a crack existence the position and geometry of this damage are revealed as a clear irregularity or discontinuity at least in some of these three isolines. Typically the rotations isolines are more sensitive and then more efficient than the deflection isolines for detecting damage. This conclusion coincides with the results shown in references [Yue85] and [PBS91]. The following figures are illustrative and they deserve some comments. The figure 1a displays the iso-

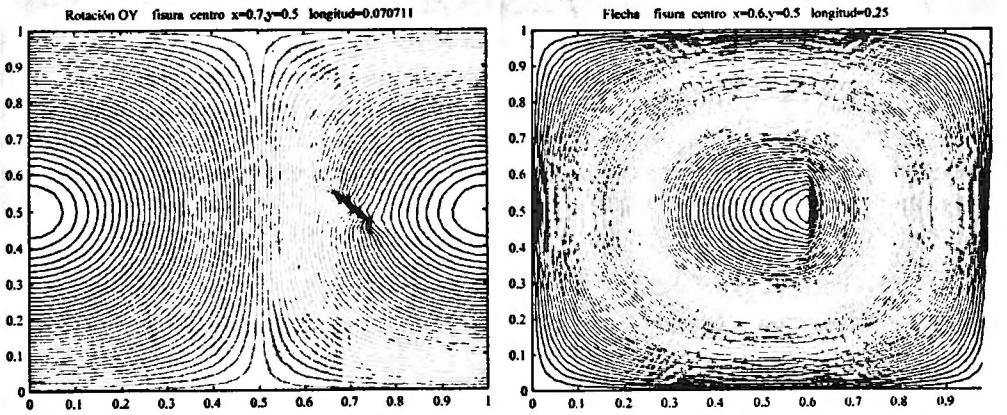

Figure 2: Modal vector 1. Plate with (a) inclined crack at $(0.7a, 0.5a)$ and length $0.07a$. Rotation θ_y isolines (b) vertical crack at $(0.6a, 0.5a)$ and length $0,25a$. Deflection w isolines

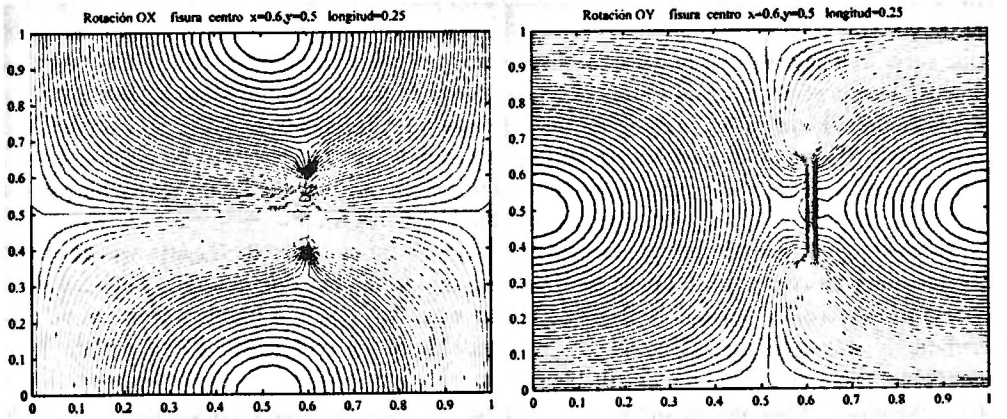

Figure 3: Modal vector 1. Plate vertical crack at $0.6a, 0.5a$ and length $0.25a$ (a) Rotation θ_x isolines (b) Rotation θ_x isolines

lines of the deflection of a plate with an inclined crack and arbitrary position. These deflection isolines do not show any type of discontinuity or difference respect an undamaged plate. However figures 1b and 2a represent the isolines of the rotations around the coordinate axis Ox and Oy. In the first figure the crack is detected in a more fuzzy way than in the second figure where the crack is clearly shown.
Analogous conclusions can be derived for other crack positions and geometry existing in a plate. In some cases deflection isolines are sufficient for the crack detection and in other situations it is necessary to recur to the other isolines, i.e. rotation isolines, more difficult to obtain than the deflection isolines, because they demand more precise measurements in the test. Figures 3a to 3b, representing rotation isolines can identify the position and existence of the crack, but also, in this case, the deflections isolines shown in figure 2b can detect the damage.

4 Metallic plates. Partially penetrating cracks

4.1 Elastic plates excited by Lamb waves

Lamb waves can be used to damage detection of partially penetrating cracks appearing in a plate. The detection of these cracks is important as they are related to structural safety. However, partially penetrating cracks are usually very difficult to observe, because they may not appear on the free faces of the plate. An excellent summary of the general theory of wave propagation is given in [LL59]. A more detailed description is presented in the recent text [RD00]. Here only final results are shown. They will be used later in a model and a numerical analysis of these surface waves.
Lamb waves corresponds a particular case of propagation of elastic waves throughout an infinite solid

that appears when the infinite solid becomes an infinite plate bounded by two free parallel faces. In this case, very often waves reflections along the faces of the plate occur and therefore the propagation of the waves modifies its direction. The wave propagation in this situation is known as guided waves.
It is assumed an homogenous and isotropic elastic plate bounded by two parallel planes separated a small distance $2h$. In figure 4 the plate and the adopted coordinate axes are shown. Then $x_2 = \pm h$ are the equations of the plate free faces and the plane (x_1, x_2), containing the normal x_3 and the direction of the wave propagation, is called sagittal plane.

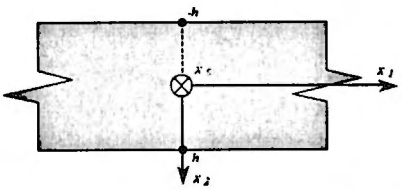

Figure 4: Isotropic plate. Coordinate axes

In the case of a thin plate in which longitudinal (L) and transversal vertical (TV) waves are propagated in its vertical plane (x_1, x_2) with successive reflections on its free surfaces $\pm h$, i. e. in this propagation there exist a coupling in material displacements with these planes. These waves are called guided waves. However, transversal (TH) waves contained in the horizontal plane x_2 are propagating only in the horizontal plane of the plate [1], because their polarization is not modified by eventual reflections and refractions. These guided waves are known as Lamb waves and they can be classified as follows: The first waves, that are propagating in the sagittal plane (x_1, x_2) are the Lamb waves L_2 and the uncoupled and polarized waves in the plane (x_1, x_3) are the Lamb TH waves.
In the following guided normal waves Lamb L_2 will be considered. Theses waves appear in a plate of thickness $2h$ comparable to the wave length, due to the existing coupling between the longitudinal L and transverse TV wave components. In this way, two types of Lamb waves can be produced. The symmetric waves (Figure 5), in which on either side of the middle plane of the plate, the longitudinal components are equal and the transverse components are opposite and the antisymmetric waves (Figure 6) in which on either side of the middle plane of the plate the transverse components are equal and the longitudinal ones opposite. The Rayleigh waves R_2, to be used in the next section, are related to the Lamb waves. They are produced when the plate thickness $2h$ is much greater than the wave length and they are propagated along the free boundary and independently of the plate thickness.

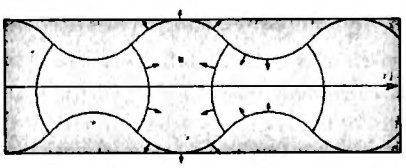

Figure 5: Lamb waves. Symmetric mode

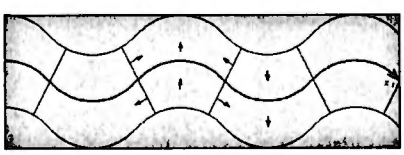

Figure 6: Lamb waves. Antisymmetric mode

According to the general theory of wave propagation, the displacement vector **u** of a material point can

[1] Similar situation occurs if a stratified plate is considered instead of the plate with its two faces free as in the text.

be derived from a potential scalar ϕ and a vector potential ψ, so that the following relation holds

$$\mathbf{u} = \nabla\phi + \nabla \times \psi \tag{2}$$

In the expression (2) the two potentials should be fulfill the two wave equations

$$\nabla^2\phi - \frac{1}{v_L^2}\frac{\partial^2\phi}{\partial t^2} = 0 \quad \text{with} \quad v_L = \left(\frac{c_{11}}{\rho}\right)^{\frac{1}{2}} \tag{3}$$

$$\nabla^2\psi - \frac{1}{v_T^2}\frac{\partial^2\psi}{\partial t^2} = 0 \quad \text{with} \quad v_T = \left(\frac{c_{44}}{\rho}\right)^{\frac{1}{2}} \tag{4}$$

with v_L and v_T are the phase velocities of the longitudinal and transverse waves. The elastic constants $c_{\alpha\beta}$, $\alpha, \beta = 1, 2, \ldots, 6$ are defined as function of the Young modulus E and the Poisson ratio ν as follows:

$$c_{11} = c_{22} = c_{33} = \frac{(1-\nu)E}{(1+\nu)(1-2\nu)} \tag{5}$$

$$c_{12} = c_{23} = c_{13} = \frac{\nu E}{(1+\nu)(1-\nu)} \tag{6}$$

$$c_{44} = c_{55} = c_{66} = \frac{E}{2(1+\nu)} = \frac{c_{11} - c_{12}}{2} \tag{7}$$

in which the remaining nonsymmetric terms $c_{\alpha\beta}$ ($\alpha \neq \beta$ are null.
As it is known the stresses and strains associated to the volume changes can be expressed in terms of the function ϕ and the stresses producing only shear deformations, without volume changes, can be expressed in terms of ψ.
It is assumed Lamb waves travel along the axis x_1 and diffraction in the x_3 is ignored. In the case of an isotropic and homogenous elastic solid the scalar and vector potentials are trigonometric functions of time t with the same frequency ω. Then, they can be expressed in the following way, with k the wave number:

$$\phi = \phi_0(x_2)e^{i(\omega t - kx_1)} \quad \text{and} \quad \psi = [\psi_{0j}(x_2)]e^{i(\omega t - kx_1)},\ j = 1, 2, 3 \tag{8}$$

A boundary value problem of the waves can be defined by the wave equations for each potential function and the boundary conditions $\sigma_{2i} = 0$, $i = 1, 2, 3$ on the free faces $x_2 = \pm h$. In order this boundary value problem can have a non trivial solution, it is necessary that the frequency ω and the wave number k satisfy the following dispersion relation, called Rayleigh-Lamb equation:

$$\frac{\omega^4}{v_T^4} = 4kq^2\left[1 - \frac{p\tan(ph+\alpha)}{q\tan(qh+\alpha)}\right] \quad \text{with} \quad \alpha = 0 \text{ and } \alpha = \frac{\pi}{2} \tag{9}$$

where the constants p and q are defined as follows:

$$p^2 = \frac{\omega^2}{v_L^2} - k^2 \quad \text{and} \quad q^2 = \frac{\omega^2}{v_T^2} - k^2 \tag{10}$$

and the angle constant α can take the values 0 and $\frac{\pi}{2}$ depending on the type of symmetry of the Lamb wave, as it will be discussed later.
If the relation (9) is satisfied, then the potencial functions can be found, except by a constant factor and their expressions are:

$$\psi_1 = \psi_2 = 0,\ \psi_3 = A\sin(qx_2+\alpha)\exp[i(\omega t - kx_1)] \text{ and } \phi = B\cos(px_2+\alpha)\exp[i(\omega t - kx_1)] \tag{11}$$

in which the constants A and B have to satisfied the following linear homogenous system of simultaneous equations:

$$\begin{bmatrix} (k^2-q^2)\cos(ph+\alpha) & 2ikq\cos(qh+\alpha) \\ 2ikp\sin(ph+\alpha) & (k^2-q^2)\cos(qh+\alpha) \end{bmatrix}\begin{bmatrix} B \\ A \end{bmatrix} = \begin{bmatrix} 0 \\ 0 \end{bmatrix} \tag{12}$$

Once the functions $\phi(x_1, x_2, t)$ and $\psi(x_1, x_2, t)$ are known, the application of formulae (2) gives the dis-

placements, except by a constant factor A, at time t of any material point (x_1, x_2) of the plate, according to the expressions

$$u_1 = qA\left[\cos(qx_2+\alpha) - \frac{2k^2}{k^2-q^2}\frac{\cos(qh+\alpha)}{\cos(ph+\alpha)}\cos(px_2+\alpha)\right]\exp[i(\omega t - kx_1)] \tag{13}$$

$$u_2 = ikA\left[\sin(qx_2+\alpha) + \frac{2pq}{k^2-q^2}\frac{\cos(qh+\alpha)}{\cos(ph+\alpha)}\sin(px_2+\alpha)\right]\exp[i(\omega t - kx_1)] \tag{14}$$

The equation (9) can be represented in the plane (ω, k) and then it defines a curve known as *dispersion curve*. In this curve three regions can be distinguished, according to the value of the phase velocity $V = \frac{\omega}{k}$ is greater either than the longitudinal wave velocity v_L or than the transverse velocity velocity v_T. Then, the relations (10) can be written as follows:

$$p^2 = \omega^2\left(\frac{1}{v_L^2} - \frac{1}{V^2}\right), \quad q^2 = \omega^2\left(\frac{1}{v_T^2} - \frac{1}{V^2}\right) \tag{15}$$

and therefore the following boundaries for the regions of dispersion space can be defined:

- Región 1.- $V > v_L > v_T$ or equivalently $k < \frac{\omega}{v_L} < \frac{\omega}{v_T}$.
  The wave numbers p and q are both real.
- Región 2.- $v_L > V > v_T$ or equivalently $\frac{\omega}{v_L} < k < \frac{\omega}{v_T}$.
  The wave numbers are q real and p imaginary.
- Región 3.- $v_L > v_T > V$ or equivalently $\frac{\omega}{v_L} < \frac{\omega}{v_T} < k$.
  The wave numbers, p and q, are both imaginary.

In the figure 7 the three regions are shown.

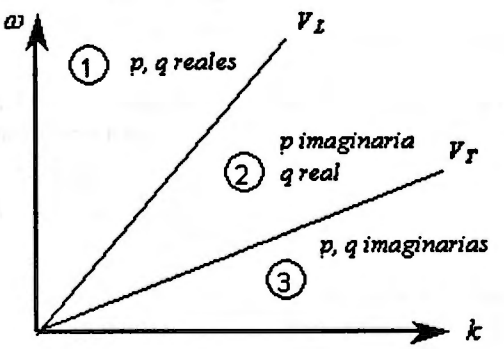

Figure 7: Rayleigh-Lamb dispersion equation. Division of the plane $\omega - k$ in three regions

For each of the three above region the corresponding expressions for the displacements when the real components of the expressions (13) and (14) are considered:

- Región 1 (p and q are real)

$$u_1 = qA\left[\cos(qx_2+\alpha) - \frac{2k^2}{k^2-q^2}\frac{\cos(qh+\alpha)}{\cos(ph+\alpha)}\cos(px_2+\alpha)\right]\cos(\omega t - kx_1)$$

$$u_2 = -kA\left[\sin(qx_2+\alpha) + \frac{2pq}{k^2-q^2}\frac{\cos(qh+\alpha)}{\cos(ph+\alpha)}\sin(px_2+\alpha)\right]\sin(\omega t - kx_1)$$

- Región 2 (p is imaginary, i.e. pi and q real)

Case $\alpha = 0$

$$u_1 = qA\left[\cos qx_2 - \frac{2k^2}{k^2-q^2}\frac{\cos qh}{\cosh ph}\cosh px_2\right]\cos(\omega t - kx_1)$$

$$u_2 = -kA\left[\sin qx_2 - \frac{2pq}{k^2-q^2}\frac{\cos qh}{\cosh ph}\sinh px_2\right]\sin(\omega t - kx_1)$$

Case $\alpha = \frac{\pi}{2}$

$$u_1 = qA\left[-\sin qx_2 + \frac{2k^2}{k^2-q^2}\frac{\sin qh}{\sinh ph}\sinh px_2\right]\cos(\omega t - kx_1)$$

$$u_2 = -kA\left[\cos qx_2 + \frac{2pq}{k^2-q^2}\frac{\sin qh}{\sinh ph}\cosh px_2\right]\sin(\omega t - kx_1)$$

- Región 3 (p and q are imaginary, i.e. pi and qi)

Case $\alpha = 0$

$$u_1 = qA\left[\cosh qx_2 - \frac{2k^2}{k^2+q^2}\frac{\cosh qh}{\cosh ph}\cosh px_2\right]\cos(\omega t - kx_1)$$

$$u_2 = -kA\left[\sinh qx_2 - \frac{2pq}{k^2+q^2}\frac{\cosh qh}{\cosh ph}\sinh px_2\right]\cos(\omega t - kx_1)$$

Case $\alpha = \frac{\pi}{2}$

$$u_1 = qA\left[\sinh qx_2 - \frac{2k^2}{k^2+q^2}\frac{\sinh qh}{\sinh ph}\sinh px_2\right]\sin(\omega t - kx_1)$$

$$u_2 = -kA\left[\cosh qx_2 - \frac{2pq}{k^2+q^2}\frac{\sinh qh}{\sinh ph}\cosh px_2\right]\sin(\omega t - kx_1)$$

A particular case of special interest of wave Lamb corresponds to the values $q^2 = k^2$. Then the equations (10) lead to the results

$$\frac{\omega^2}{v_T^2} = 2k^2 \quad \rightarrow \quad V = \frac{\omega}{k} = v_T\sqrt{2} \tag{16}$$

i.e., as the following relations $v_L > V > v_T$ are satisfied, the dispersion curve is in the region 2, and then p is imaginary ($p = \chi i$). Moreover the plate velocity V_P fulfills the condition

$$V_P = v_T\sqrt{2}\sqrt{1+\frac{c_{12}}{c_{11}}} > v_T\sqrt{2} \tag{17}$$

where the plate velocity V_P is the limit of phase velocity when the frequency ω and k, both approach to zero in a Lamb wave symmetric mode. The equation (17) is valid for every mode except for the antisymmetric mode, represented by A_0, with a velocity V smaller than v_T.
In general, when $q = k$ it can be written $kh = \frac{n\pi}{2}$ with n odd for symmetric modes and even for antisymmetric modes. The Lamé modes appear for equally spaced values of the frequency-thickness product, given by the formula

$$2hf = n\frac{v_T}{\sqrt{2}}, \quad n = 1, 2, \ldots$$

In figure 8a the variations of u_1 and u_2 throughout the plate thickness for the symmetric mode S_0 is shown. The displacement u_1 is null along the plate faces because the Lamb wave is simply a TV wave, i.e. a transverse wave polarized in the sagittal plane x_1x_2. As it can be observed in figure 8b this mode is propagating, along the plate axis x_1, with an angle $\frac{\pi}{4}$ respect to the axis x_1, such that $V = v_T\sqrt{2}$.

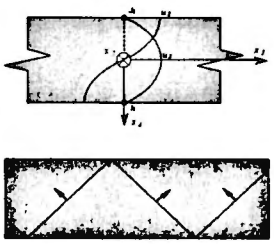

Figure 8: Lamb wave (Lamé mode) for $q^2 = k^2$. (a) Propagation to 45° (b) Displacements

4.2 Numerical simulation. Application

A illustrative example of the application of the Lamb waves as a tool to identify partially penetrating cracks in metallic plates an laboratory test will be numerically simulated.

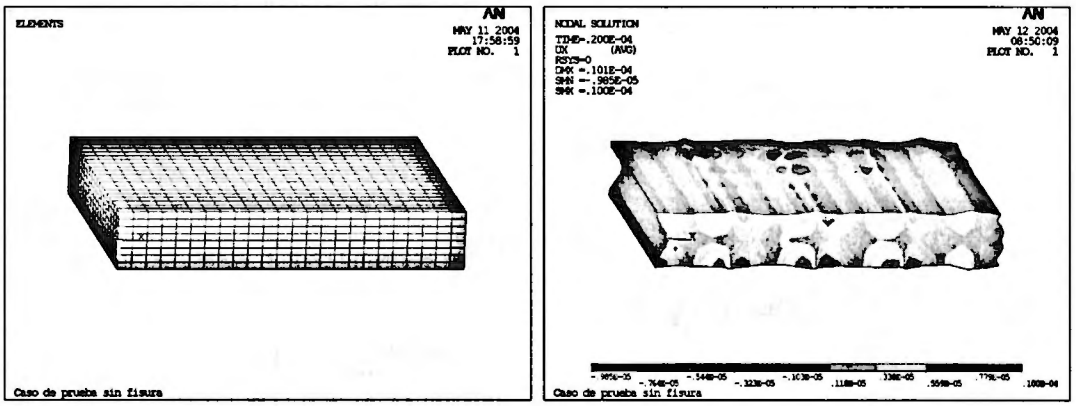

Figure 9: Uncracked plate. (a) FE mesh. (b) Displacements u_1 at $t = 2.5 \times 10^{-5}$ sec

In the following a rectangular steel plate of the following dimensions is considered. Total thickness $2h = 0.02$ m, plan dimensions $a = 0.200$ m and $b = 0.120$ m. A train of symmetric Lamb waves ($\alpha = 0$ of frequency $f = 200 \times 10^3$ Hz is introduced in the plate trough the side of length a. The material of the plate has the following characteristics: Young modulus $E = 1.962 \times 10^8$ MPa, Poisson ratio $\nu = 0.3093$ and density $\rho = 7.797$ t/m^3. From these data the angular frequency is $\omega = 1256637.061$ rad/sec, the transverse and longitudinal velocities are: $v_T = 3099.9248$ m/sec and $v_L = 5889.5724$ m/sec and from the dispersion equation the wave number is $k = 218.1658$ m^{-1} and the wave velocity is $V = 5760.01$ m/sec are obtained. In this particular case the Lamb wave is situated in the region 2, i.e. p is an imaginary number and p is a real one.

Using the properties of symmetry of the analysis half plate has been modelled. The FE mesh has been uniform with 24 divisions along the longitudinal direction x_1, 8 divisions along direction x_2 and 20 through the thickness (direction x_3). The the maximum side length of an element is 0.005 m and the time increment used was 120 per cycle i.e. $\Delta t = 4,17 \times 10^{-8}$ sec. The FE mesh used in the analysis is shown in figure 9a.

The displacement results of the wave propagation analysis for a particular time are shown in figure 9b.

Similar procedure has been carried out on a damaged plate with a crack parallel to side a and situated at section $x_1 = 0.007$ m. The total length of the crack was 0.010 m and its depth was 0.010. The constant crack width was 0.002 m. The mesh and the results are shown in figures 10a and 10b. It can be observed that the dimensions and position of the crack are directly revealed in this analysis[2].

[2]In this preliminary analysis it has not been considered the possible impact-contact between the two faces of the crack

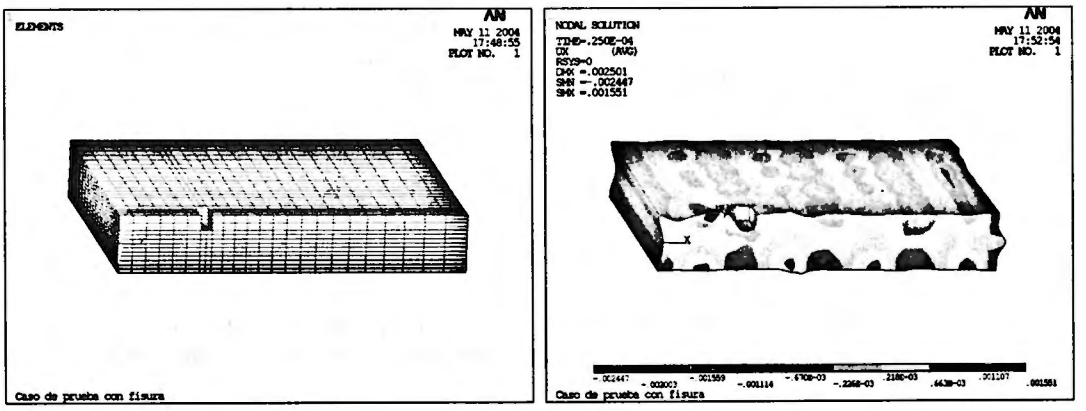

Figure 10: Cracked plate. (a) FE mesh. (b) Displacements u_1 at $t = 2.5 \times 10^{-5}$ sec

5 Metallic plates. Superficial cracks

5.1 Elastic plates excited by Rayleigh waves

Rayleigh waves can be used to damage detection of superficial cracks appearing in a plate. Typically, the detection of these superficial cracks or fissures is important due to their relation to structural maintenance and protection rather than to safety requirements. Details of this approach for damage identification can be seen in [SM02], and therefore only main results will given below.

The Rayleigh waves represent a particular case of elastic waves propagating along a free surface of an infinite half space elastic solid without penetrate into it.

The coordinate cartesian axis are Ox_i, $i = 1, 2, 3$ and the infinite half space elastic solid is defined by the domain $x_3 < 0$. The waves are propagated along the boundary plane $x_3 = 0$ in the direction Ox_1. The problem to be solved is a 2-D elasticity, namely in plane strain and therefore only the plane $x_2 = 0$ is considered, i.e. the one containing the coordinate axis Ox_1x_3.

The waves equation for each component u of the displacement vector, either longitudinal, $\mathbf{u}_l$, or transversal, $\mathbf{u}_t$, is the following one[3]:

$$\frac{\partial^2 u}{\partial t^2} - c^2 \Delta u = 0 \tag{18}$$

where $c = v_L$ or $c = v_T$ is the respective wave propagation velocity according to the component u is a component of the displacement vector $\mathbf{u}_l$ or of the vector $\mathbf{u}_t$.

The solution of (18) is assumed to be in the form:

$$u = e^{i(kx_1 - \omega t)} f(x_3) \tag{19}$$

that if it is introduced into equation (18) this one becomes:

$$\frac{d^2 f}{dx_3^2} = \left(k^2 - \frac{\omega^2}{c^2}\right) f(x_3) \tag{20}$$

If $k^2 - \dfrac{\omega^2}{c^2} < 0$ then the periodic wave is not damped inside the elastic solid and the waves are not belonging to the superficial type. Then it is assumed that the condition holds: $k^2 - \dfrac{\omega^2}{c^2} > 0$ and the following result is obtained after integration of (20):

$$f(x_3) = Ce^{\pm x_3 \sqrt{k^2 - \frac{\omega^2}{c^2}}} \tag{21}$$

[3]For completeness, now the wave propagation solution will be obtained by taken as basic unknowns the displacements instead of the potential functions, as it was done in the Lamb wave propagation analysis

It should be noticed that for $x_3 \to -\infty$ it must $f(x_3) \to 0$ and introducing the parameter[4] $\mu = \sqrt{k^2 - \frac{\omega^2}{c^2}}$ the expression (21) becomes into the following one:

$$f(x_3) = Ce^{\mu x_3} \tag{22}$$

and then each component of the longitudinal and transversal wave displacement given by (19) becomes:

$$u = Ce^{i(kx_1 - \omega t)}e^{\mu x_3} \tag{23}$$

The real displacement vector is the sum of the vectors $\mathbf{u}_l$ and $\mathbf{u}_t$ and their components satisfy the equation (18) with $c = v_L$ or $c = v_T$ according to the respective case. The linear combination of both waves is found using the condition that the resultant stresses are zero along the free boundary $x_3 = 0$, i.e. along the boundary limiting the elastic solid. Mathematically this condition can be expressed by the following equation:

$$\sigma_{ij} n_j = 0$$

in which the index summation convention is assumed and $\mathbf{n} = (n_i)$ is the unit vector normal to the boundary, in this case this vector is $\mathbf{n} = (0, 0, 1)$.
Due to the fact that the problem under consideration is a 2-D initial-boundary value problem of the total displacement vector $\mathbf{u} = \mathbf{u}(x_1, x_3)$ and free boundary conditions at the face $x_3 = 0$ of the plate, i.e. the values for three components of the stress tensor at :

$$\sigma_{13} = \sigma_{23} = \sigma_{33} = 0$$

Using a similar procedure as in previous section, but now with the displacements the basic unknowns, that have to satisfy the equilibrium, constitutive and compatibility equations, the following final results related to the Rayleigh waves are obtained:
The relation between the frequency ω and the wave number k or dispersion equation is obtained as the condition of existence of a non trivial solution of the initial-boundary value problem. Its expression is

$$(k^2 + p^2)^2 = 4k^2 pq \tag{24}$$

The condition (24) can be substituted by the following equivalent more convenient equation:

$$\xi^6 - 8\xi^4 + 8(3 - 2\lambda^2)\xi^2 - 16(1 - \lambda^2) = 0 \tag{25}$$

with the notation ξ and λ for the ratios $\frac{V}{v_T}$ and $\frac{v_T}{v_L}$ respectively, i.e

$$\xi = \frac{\omega}{v_T k}, \quad \lambda = \frac{v_T}{v_L} = \sqrt{\frac{1 - 2\nu}{2(1 + \nu)}}$$

and p and q are now denoting the imaginary parts of the roots p and q. The unknown ξ can be found as a root of the equation (24).
As the frequency of the superficial, transversal and longitudinal, waves is proportional to the wave number with a proportionality constant equal to the wave propagation velocity V, then the following equality is obtained: $V = v_T \xi$.
Using the following equations the constants p and q are found:

$$p = \sqrt{k^2 - \frac{\omega^2}{v_T^2}} = k\sqrt{1 - \xi^2}, \quad q = \sqrt{k^2 - \frac{\omega^2}{v_L^2}} = k\sqrt{1 - \lambda^2 \xi^2} \tag{26}$$

Finally the componentes of the transversal $\mathbf{u}_T$ and longitudinal $\mathbf{u}_L$ displacement vectors can be obtained

[4]Tha parameter μ takes the values ip or iq depending on the velocity c is v_L or v_T respectively

by using the following expressions:

$$u_{t1} = -k(2-\xi^2)\sqrt{1-\xi^2}e^{k[ix_1-iVt+\sqrt{1-\xi^2}x_3]} \quad (27)$$

$$u_{t3} = ik(2-\xi^2)e^{k[ix_1-iVt+\sqrt{1-\xi^2}x_3]} \quad (28)$$

$$u_{l1} = 2k\sqrt{1-\xi^2}e^{k[ix_1-iVt+\sqrt{1-\lambda^2\xi^2}x_3]} \quad (29)$$

$$u_{l3} = -2ik\sqrt{1-\xi^2}\sqrt{1-\lambda^2\xi^2}e^{k[ix_1-iVt+\sqrt{1-\lambda^2\xi^2}x_3]} \quad (30)$$

A last observation about the dispersion equation. It should aware that among the solutions of the equation (25) only the ones satisfying the inequality $0 \leq \xi \leq 1$ should be considered, because by definition ξ is positive and the constants p and q are real. Besides, it is convenient to observe that λ fulfill the condition $0 \leq \lambda \leq \frac{1}{\sqrt{2}}$ and therefore only one solution of the equation (25) exists with these characteristics that is within the interval $0,874 \leq \xi \leq 0,955$. Also it is noticed that for depths greater than twice the wave length, i.e. for depths $x_3 < -\frac{2}{k}$ the displacements are negligible, or equivalently, most of the wave energy is concentrated along the surface of the elastic solid.

5.2 Numerical simulation. Application

In the numerical simulation of elastic waves several techniques are currently used: Finite differences (FD), Finite elements (FE) and Boundary elements (BE). Each of them has pros and cons. In this work a scheme in finite differences in the temporal discretization and the finite element method for spatial discretization of the continuous model was applied.

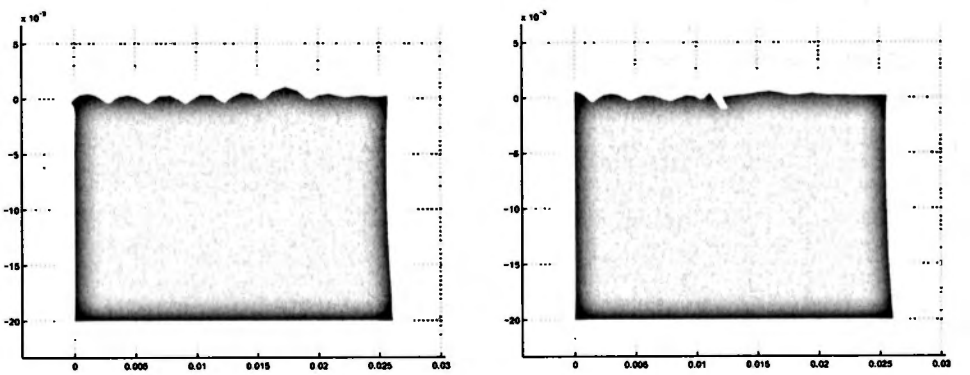

Figure 11: (a) Undamaged plate (b) Damaged plate with a rectangular micro-crack

Using the advantage of the FE a very refined mesh has been used in the boundary region near the crack where its geometry should be reproduced with detail and also along the superficial boundary of the elastic solid, zones with high gradient of stresses produced by the travelling Rayleigh waves. Isoparametric bilinear finite elements have been used with interpolation at the vertices of the quadrilateral elements. A 4×4 Gauss integration formula has been considered in the FE matrices numerical evaluation. The spatial discretization leads to a system of a large number of simultaneous ordinary differential equations. In order to increase the accuracy of the solution and eliminate the dissipative and dispersive effects inherent to some FD schemes an implicit unconditionally stable scheme of second order has been chosen. The selected FD scheme is the trapezoidal rule, that belongs to the Newmark family of FD methods with the parameters $\beta = \frac{1}{4}$ and $\gamma = \frac{1}{2}$.

This numerical technique has been applied to the simulation of a laboratory test carried out on a aluminium plate of dimensions in plan 130×400 mm and thickness 20 mm. The plate material characteristics are the following ones: $E = 7,41 \times 10^{10}$ N/m^2, $\rho = 2,7 \times 10^3$ kg/m^3 and $\nu = 0,3302$. The wave number assumed was $k = \frac{2\pi}{3} \times 10^3$ m^{-1}.

Using these data the following intermediate results have been obtained:

$$\begin{aligned} v_L &= 6379,07\,\text{m/seg}, \quad v_T = 3211,84\,\text{m/seg} \\ \lambda &= \frac{v_T}{v_L} = 0,503496, \quad \xi = 0,932053 \\ U &= 2923,61\,\text{m/seg}, \quad \omega = 6269791,88\,\text{rad/seg}, \quad f = 997869\text{Hz} \end{aligned}$$

The results corresponding to the study of a undamaged plate and the same plate but damaged with a rectangular micro-crack of dimensions: width $6,933 \times 10^{-4}$ m and depth $1,25 \times 10^{-3}$ m are presented. Due to the test characteristics and in order to diminish the computational effort only one fifth of the total plate length but keeping the plate depth, i.e. the model dimensions were: $L_1 = 0.026$ and $L_3 = 0.020$ metros.
The FE mesh used in this analysis was composed by 1891 nodes and 1900 elements. The proportion between the numbers of elements in vertical and horizontal direction has been selected nearly equal to the ratio between the height and the length of the model. The mesh has been also refined at the neighborhood of the boundary $x_1 = 0$. The time step size was $\Delta t = 2 \times 10^{-8}$ and the maximum simulated time span time was $T = 3 \times 10^{-6}$.
The computer time was 2460 CPU seconds in a Pentium III of 500 MHz computer.
In figures 11a and 11b the behavior of the Rayleigh waves in the damaged and undamaged plates is presented. It can be observed the even very small cracks are immediately detected because the Rayleigh waves stop their travel when they found the obstacle represented by the micro crack. It is expected that for a 3-D model this property can be used to identify no only the existence of the damage but also its geometry and localization in plan. This type of tests will permit to maintain the quality of protective painting of plates.

6 Reinforced concrete beams

The discussion in the following parts of this section 6 is concentrated to detection methods of damage in reinforced concrete structures, i.e. to crack identification of structures composed by beams, although some comments can be extended and applied to other more complex structures. Evidently, this issue is a different topic respect to metallic structures damage detection previously described. This difference is due to the non homogeneity of the reinforced concrete and the fact that typically the identification procedure is carried on the already built structures. These circumstances prevent the application of the previously described damage detection methods (use of guided waves and partial dynamic structural excitation etc.) to the civil and building structures. Very often these structures are excited to low frequencies vibrations.
As it is well known health monitoring of reinforced concrete beams by using dynamic tests has been a topic of intensive research for the last decades. Typically they are based on the estimation of the changes of a selected dynamic characteristic of the cracked structure, i.e. of a Dynamic System Characteristic (DSC), either natural frequencies, or mode shapes or measured of the dynamic flexibility, in comparison to the uncracked one. A short summary of the use of these DSCs in the damage detection methodology is given. The inherent models for the cracked beam behavior are also discussed. Currently, the effect of cracking in the free vibrations of a concrete beam is analyzed according to one of the following three approaches. In the first approach it is assumed that the cracks width and pattern remain unchanged during the beam vibration. In the second approach a bilinear behavior for the beam is considered, namely, the beam behaves as uncracked or as cracked depending on the crack is closing or is opening respectively. Finally, the third approach uses a time dependent model in order to replicate the variation of the closure and opening of the cracks by the introduction of a set of discrete springs. Most of the detection damage models for reinforced concrete beams uses the first approach, that implies the fulfillment of the following assumption: the beam vibrates with small amplitudes around cracked static equilibrium states. This hypothesis can be accomplished in many dynamic tests of structures in the field. However, despiste of this fact recent contributions considering the nonlinear concrete behavior has been published [Rab01] and [MFH+90].
This section is finished by a comparative study among the different DSCs commonly used. It can be observed that, in general, differences between uncracked and cracked beams are small and some they can not be distinguished from the inherent measurement errors occurring during the tests.
In the nest section 7 the simple linear elastic model of cracked beams initially developed by [CB84] is summarized. The model is extended from the original case of a single symmetric crack in a beam to

multiple and non symmetric cracks in order to cope more realistic situations. Finally, some comments about the identification methodology are also given.

6.1 Dynamic system characteristics

In general, the crack presence in a structure reduces its natural frequencies and increases its damping respect to the uncracked structure. By comparing the results of these DSCs obtained in the pristine structure (or in a theoretic model, usually in FE) and the ones found in a dynamic test in the cracked structure is ideally possible by comparison to detect the presence of structural damage, crack position and severity. This identification process implies to solve an inverse problem, that demands previously the construction of a structural model for the dynamic behavior of the damaged structure. A very simple model of this type is to reduce the elasticity modulus do the damaged elements of the structure, although there exist more realist alternative models, in which the crack presence is better simulated.
In important point in a damage detection method is the selection of DSC to be compared. In the following the merits and drawbacks of some possible choices are discussed. In this respect different DSCs have been used. For example, in addition of the reduction of the natural frequency and the modification of modal shapes o their derivatives, the response function in the frequency domain, wavelet transforms and the power spectral density, among others have been analyzed. Also in same occasions a multiple criteria for damage detection has been applied, in which several DSCs has been considered. Obviously, the selection of the DSC depends in each case on the identification procedure used, as error minimization, penalty function, use of genetic algorithms [ASM04], neuronal networks approximation [KH03] etc.

6.2 Natural frequencies

Measurement of natural frequencies is an inexpensive and quick procedure for structural damage detection. One advantage of this DSC is its global character, because any localized crack in the structure can be in principle revealed by this measurement. However, the sensitivity of the frequency to the damage may depend on the its severity and its localization. For example, if the crack is concentrated near a node of the vibration mode of the natural frequency, then the stress modification produced by the crack presence is very small. Then the damage sensitivity for the natural frequency considered is very low. Contrary conclusion results, if the damaged area coincides with the modal crest. Summarizing, damage represents a stiffness reduction and therefore a decrease of the natural frequency. Moreover, if damage increases, either in number of cracks or in their severity, also the natural frequency diminishes.
Normally, small cracks can not be detected easily, because the difference between natural frequencies of the undamaged and damaged structures is very small and it may be originated by other causes (temperature, traffic noise, measurement accuracy etc.). Therefore, it is usual to admit cracks existence if the difference is greater than 5 %. However, it is possible to measure natural frequencies at different phases along the life of the structure, and in this way, to evaluate the damage degree, or at least its progression, if damage already exists and differences are increasing with time. Sometimes, the measured frequencies are greater than the theoretical ones. In these cases there exist an increase of the structure stiffness, usually in its supports.
An aspect to be considered when frequencies are used as DSC is referred to the choice of its most suitable order. There is a lack of consensus on this point. Low order frequencies are simple and easy to obtain in a test. However high order frequencies generate complex modes of vibration, suitable to detect damage. Related to this issue is the selection of the frequencies number to use in the test and in the damage identification algorithm.
An important limitation of the use of this DSC is to assume a particular structural damage, a crack, that is modelled by a hinge. This model prevents the identification of other types of damage, as steel corrosion, that does not modify significatively the natural frequency of the structure. Similar comment can be applied to structural damage caused by stress losses in prestress tendons, unless in the dynamic tests on the undamaged and damage structures an additional accompanying load is introduced in order to reveal this type of damage. Finally in symmetric structures the computed damage position may be not be unique.
Summarizing, the damage detection method based on frequency measurements is of limited application, because a special type of damage and a structural geometry are assumed. Typically, only the few first frequencies are tested and in this case the test is simple and inexpensive. Frequently these dynamic tests should be accompanied with other complementary tests in order to reach reliable identification results. An excellent review of this identification technique is given in [Sal97].

The relation between the changes of the stiffness of the structure and the natural frequencies can be found by using the shape vibration modes of the uncracked structures as follows:
Let it be ω_i and ϕ_i the natural frequency and the corresponding mode of vibration of order i. It is assumed that the mode is normalized respect to the mass matrix $\mathbf{m}$ of the uncracked structure, i.e. the following condition is satisfied:

$$\phi_i^T \mathbf{m} \phi_i = 1 \tag{31}$$

In addition, each mode i is solution of the equation

$$\mathbf{k}\phi_i = \lambda_i \mathbf{m}\phi_i \quad \text{with} \quad \lambda_i = \omega_1^2 \tag{32}$$

and by pre-multiplying by ϕ_i this equation becomes:

$$\phi_i^T \mathbf{k} \phi_i = \lambda_i \phi_i^T \mathbf{m} \phi_i = \lambda_i \tag{33}$$

The stiffness matrix $\mathbf{k}$ of the pristine structure is modified to the matrix $\mathbf{k}^d$ of the damage structure, that can be written, $\mathbf{k}^d = \mathbf{k} + \delta\mathbf{k}$ and it is assumed that damage does not modify the mass matrix of the structure.
The new modes of vibration of the damage structure should satisfy the normalizing condition (31), that is simplified in the following expression, if second order terms are neglected.

$$(\phi_i + \delta\phi_i)^T \mathbf{m}(\phi_i + \delta\phi_i) = 1 \rightarrow \delta\phi_i^T \mathbf{m}\phi_i + \phi_i^T \mathbf{m}\delta\phi_i = 0 \rightarrow \phi_i^T \mathbf{m}\delta\phi_i = 0 \tag{34}$$

The above equation can be written in the following way:

$$(\mathbf{k} + \delta\mathbf{k})(\phi_i + \delta\phi_i) = (\lambda_i + \delta\lambda_i)\mathbf{m}(\phi_i + \delta\phi_i) \rightarrow \mathbf{k}\delta\phi_i + \delta\mathbf{k}\phi_i = \lambda_i \mathbf{m}\delta\phi_i + \delta\lambda_i \mathbf{m}\phi_i \tag{35}$$

and pre-multiplying by ϕ_i^T and using the relation $(\phi_i + \delta\phi_i)^T(\mathbf{k} + \delta\mathbf{k})(\phi_i + \delta\phi_i) = \lambda_i + \delta\lambda_i$ the final expression that relates the frequency change $\delta\lambda_i$ in terms of the changes of the stiffness matrix

$$\delta\lambda_i = \phi_i^T \delta\mathbf{k} \phi_i \tag{36}$$

It is a common hypothesis to express the stiffness matrix of the damage structure in terms of the distinct element matrices affected by a factor, β_j, called damage coefficient, that reduces the elasticity modulus of the damaged element j, i.e

$$\mathbf{k}^d = \sum_{j=1}^{m} \beta_j \mathbf{k}_j \tag{37}$$

with m the number of elements that can be potentially damaged and $0 \leq \beta_j \leq 1$.

6.3 Frequencies and static test data

The damage detection based on static tests are simpler than the ones based on dynamic tests, because the static equilibrium equations stiffness is the relevant property. Moreover, the costs of the dynamic test are higher than the ones of a static test.
Some damage detection methods uses hybrid tests as in [WHFY01]. In this work the damage identification is carried out in two phases. In the first the changes of natural frequencies are used and afterwards the displacements of the structure are measured under different static loading cases. With these two groups of data and the tentative assumption of equal severity of damage it is possible to identify the damaged zone of the structure,. Then, once the damaged zone has been tentatively identified the intensity of the damage can be estimated.
The main idea of this combined damage identification method consists to test the structure under several loads combination. The damage identification uses the comparison between the measured static displacements and the frequencies in the undamaged and in the damaged structure. For both groups of results the changes due to the damage is computed using a first order approximations as follows:

- Static displacements $\mathbf{u}$ in the undamaged structure

$$\mathbf{ku} = \mathbf{p} \rightarrow \mathbf{u} = \mathbf{k}^{-1}\mathbf{p} \tag{38}$$

- Static displacements $\mathbf{u}^d$ in the damaged structure

$$\mathbf{k}^d\mathbf{u}^d = \mathbf{p} \rightarrow \mathbf{u} = (\mathbf{k} + \delta\mathbf{k})^{-1}\mathbf{p} \approx (\mathbf{k}^{-1} - \mathbf{k}^{-1}\delta\mathbf{k}\mathbf{k}^{-1})\mathbf{p} \tag{39}$$

then

$$\delta\mathbf{u} = \mathbf{u} - \mathbf{u}^d = \mathbf{k}^{-1}\delta\mathbf{k}\mathbf{k}^{-1}\mathbf{p}$$

and the damaged matrices are affected by the corresponding damage factors β. Similarly, the natural frequency can be evaluated according (36).
Several identification algorithms,[HS97] and [SS91], for damaged elements, that use the minimization of an objective function of quadratic error type have been used in applications. However, two main sources of errors exist in the static tests. (1) The information from a static test is more scarce than a dynamic test, and therefore it makes more difficult to obtain reliable results in the identification procedure. (2) The damage effects can be cancelled due to the limited number of load paths. For example, an existing damage can not be revealed for a particular load case, if its effect is small in the global deformation of the structure. In order to avoid these difficulties several alternative procedures have been developed, that can generate automatically the load cases to be tested, in such a way that potential damages can be detected.

6.4 Frequencies and mode shape derivatives

An important point in damage identification is to establish a correct correlation between the DSCs measures from the test and the damage existence, localization and severity. In general any local or global damage is associated to structural changes, that can be observed through changes in the DSCs.
In addition to natural frequencies as DSCs another damage indication can be the direct comparison between modes, or their first derivatives or in some cases their curvatures. The main difficulty in this approach lies on a suitable selection of the order of the modes used to reveal the damages or, in the case of first derivatives and curvatures of modes, on the ability to obtain a sufficiently accurate measure of these DSCs. In [DT04] a numerical simulation using curvatures and natural frequencies computed by EF with error estimation and re-meshing techniques to improve the solution have been presented
Then, several methods have been proposed to establish the former correlation. Some of them, with reference to reinforced concrete beams, are commented below.

- Modal Assurance Criterion (MAC) and Coordinate Modal Assurance Criterion ($COMAC$).

  These derived values from the DCSc are defined by the expressions

$$MAC_{jk} = \frac{|\sum_{i=1}^{n}(\phi_{Ai}^{j})(\phi_{Bi}^{k})|^2}{\sum_{i=1}^{n}(\phi_{Ai}^{j})^2 \sum_{j=1}^{n}(\phi_{Bi}^{k})^2}, \qquad COMAC_i = \frac{|\sum_{j=1}^{m}(\phi_{Ai}^{j})(\phi_{Bi}^{j})|^2}{\sum_{j=1}^{m}(\phi_{Ai}^{j})^2 \sum_{j=1}^{m}(\phi_{Bi}^{j})^2} \tag{40}$$

  in which $\Phi_A = [\phi_A^j]$ with $j = 1, 2, \ldots, m_A$ the matrix of $n \times m_A$ dimension, containing the m_A modes od vibration that have considered in the test A and similarly the matrix $\Phi_B = [\phi_A^k]$ of dimension $n \times m_B$ of the test B is defined. The components of the mode, ϕ_A^i, column vector of dimension n, are written as $\phi_A^i = (\phi_{Ai}^j)$ with $i = 1, 2, \ldots, n$ and similarly for the test B. In the expression of $COMAC$ it was assumed the existence of m vibration modes common for both tests.

  The value of MAC varies between 0 and 1. If $MAC = 1$ then there exists a total correlation between both tests and when this value approaches to zero means there is structural damage.

  The value $COMAC$ is often used to identify the structural mode from two sets of measurements do not correlate. Values close to 1 show a correlation for the modal coordinate i and small values are indication od damage existence.

- Method of strain energy.

  As it is well known the strain energy produced by a mode $\phi_i(x)$ in a beamlike structure of span L and section of bending stiffness $EI(x)$ can be computed either directly or as sum of the strain

energy of N finite elements, that divide its length, according to the expression:

$$U_i = \int_0^L EI(x)\left(\frac{\partial^2\phi_i}{\partial x^2}\right)^2 dx = \sum_{j=1}^{N} U_{ij} \quad \text{with} \quad U_{ij} = \int_{a_j}^{a_{j+1}} EI_j\left(\frac{\partial^2\phi_i}{\partial x^2}\right)^2 dx \tag{41}$$

For each element it can be defined its proportion of strain energy respect to the total strain energy of the beam by the following formula:

$$F_{ij} = \frac{U_{ij}}{U_i} = \frac{EI_j f_{ij}}{\overline{EI} f_i} \quad \text{with} \quad \sum_{j=1}^{N} F_{ij} = 1 \tag{42}$$

in which the average stiffness of the element j and the average stiffness of the beam are denoted by EI_j and $\overline{EI}$ respectively.

The variables related to the damaged beam are identified by the superscript d and the following relations can be written:

$$\frac{EI_k}{EI_k^d} = \frac{\dfrac{f_{ik}^d}{f_i^d}}{\dfrac{f_{ik}}{f_i}} = \frac{\overline{f}_{ik}^d}{\overline{f}_{ik}} \tag{43}$$

In order to use the m vibration modes considered in the test it is defined the damage index for the element k as follows:

$$\beta_k = \frac{\sum_{i=1}^{m} \overline{f}_{ik}^d}{\sum_{i=1}^{m} \overline{f}_{ik}} \tag{44}$$

The damage index gives an indication about the health of a structure, because β_k represents the deterioration degree of the bending stiffness of element k due to the change of the stored energy in the structure caused by a particular vibration mode. It is assumed that the indexes β_k represent a random variable with normal distribution. Then it is possible to define a normalized damage index as:

$$z_k = \frac{\beta_k - \overline{\beta_k}}{\sigma_k} \tag{45}$$

with $\overline{\beta_k}$ and σ_k are the mean and standard deviation of the damage index population.

- Method of the flexibility

The presence of a damage in a structure increases its flexibility. Then, based on this fact it is possible to compute the flexibility matrix of a structure from the knowledge of its n vibration modes measured in the tests. These modes are assumed to be normalized respect to the mass matrix, $\mathbf{m}$, i. e. they fulfill the condition for $i = 1, 2, \ldots, n$:

$$\boldsymbol{\phi}_i^T \mathbf{m} \boldsymbol{\phi}_i = 1$$

The stiffness matrix $\mathbf{k}$ and the flexibility matrix $\mathbf{f}$ of the system are:

$$\mathbf{k} = \mathbf{m}\boldsymbol{\phi}\boldsymbol{\Omega}\boldsymbol{\phi}^T\mathbf{m} \approx \mathbf{m}\left(\sum_{i=1}^{n} \omega_i^2 \boldsymbol{\phi}_i \boldsymbol{\phi}_i^T\right)\mathbf{m} \rightarrow \mathbf{f} = \boldsymbol{\phi}\boldsymbol{\Omega}^{-1}\boldsymbol{\phi}^T \approx \sum_{i=1}^{n} \frac{1}{\omega_i^2}\boldsymbol{\phi}_i\boldsymbol{\phi}_i^T \tag{46}$$

where $\boldsymbol{\phi}$ is the matrix containing the n modesas column vectors and $\boldsymbol{\Omega} = \text{diag}(\omega_i^2$.

Therefore, if $\mathbf{f}$ and $\mathbf{f}^d$ are the flexibility matrices of the pristine and damaged structures respectively, then the following matrix damage indicator $\Delta\mathbf{F}$ can be defined as the difference

$$\Delta\mathbf{F} = \mathbf{F} - \mathbf{F}^d \tag{47}$$

Each column of $\Delta\mathbf{F}$ corresponds to locations of the test measurements in the structure. The

damage identification and its location is carried out according to the maximum values of each column of the matrix.

- Method of the residual dynamic forces

  Finally, there exist other procedures that use the modal measurements of the test in a different way than standard methods in order to obtain, for example, the residual dynamic forces. Then it is possible to define a new objective function to be minimaze in the damage identification process. This interesting concept expresses the dynamic equilibrium that should satisfy a structure subjected to free vibrations. This procedure will be summarized in the following.

  The displacements of an undamped structure with n degrees of freedom is governing by the system of differential equations

$$\mathbf{m\ddot{u}} + \mathbf{ku} = \mathbf{0} \tag{48}$$

  and for the natural frequency of order i the following equation is satisfied

$$\mathbf{k}\boldsymbol{\phi}_i - \omega_i^2 \mathbf{m}\boldsymbol{\phi}_i = \mathbf{0} \tag{49}$$

  When damage occurs the matrix of the uncracked structure $\mathbf{k}$ becomes into $\mathbf{k}^d$. As it has been already discussed, expression (37) this matrix can be expressed as sum of the element matrices, each multiplied by a damage coefficient β_j, i. e.

$$\mathbf{k}^d = \sum_{j=1}^{m} \beta_j \mathbf{k}_j \tag{50}$$

  with m the number of potentially damaged elements and $0 \leq \beta_j \leq 1$

  Assuming the mass matrix remains constant if damage occurs and the corresponding frequencies and modes of the damaged structure satisfied the following equations, for each frequency:

$$\mathbf{k}^d \boldsymbol{\phi}_i^d - (\omega_i^d)^2 \mathbf{m}\boldsymbol{\phi}_i^d = \mathbf{0} \tag{51}$$

  From the former equations the residual dynamic force vector for the mode i, can be expressed approximately:

$$\mathbf{R}_i = -(\omega_i^d)^2 \mathbf{m}\boldsymbol{\phi}_i^d + \sum_{j=1}^{m} \beta_j \mathbf{k}_j \boldsymbol{\phi}_i^d \tag{52}$$

  The vector of equation (52) will be zero if the correct values of the damage coefficients β_j at each element j are introduced and the exact information about the values of the frequency ω_i^d and the mode vector $\boldsymbol{\phi}_i^d$ of order i as well. This equation is valid for all frequencies and modes $(i = 1, 2, \ldots, n)$ and al of then can be written explicitly in the following way:

$$\begin{bmatrix} R_{1i} \\ R_{2i} \\ \cdot \\ \cdot \\ \cdot \\ R_{ni} \end{bmatrix} = \begin{bmatrix} k_{11}^d - (\omega_i^d)^2 m_{11} & k_{12}^d - (\omega_i^d)^2 m_{12} & \ldots & k_{1n}^d - (\omega_i^d)^2 m_{1n} \\ k_{21}^d - (\omega_i^d)^2 m_{21} & k_{22}^d - (\omega_i^d)^2 m_{22} & \ldots & k_{2n}^d - (\omega_i^d)^2 m_{2n} \\ \cdots & \cdots & \cdots & \cdots \\ \cdots & \cdots & \cdots & \cdots \\ \cdots & \cdots & \cdots & \cdots \\ k_{n1}^d - (\omega_i^d)^2 m_{n1} & k_{n2}^d - (\omega_i^d)^2 m_{n2} & \ldots & k_{nn}^d - (\omega_i^d)^2 m_{nn} \end{bmatrix} \begin{bmatrix} \phi_{1i} \\ \phi_{2i} \\ \cdot \\ \cdot \\ \cdot \\ \phi_{ni} \end{bmatrix} \tag{53}$$

  It can be shown that the terms R_{ii} are zero if the matrices $\mathbf{k}_d$ and $\mathbf{m}$ are real and symmetric, and then from the former results is possible to build the following objective function to be minimized:

$$f(\beta_1, \beta_2, \ldots, \beta_n) = \sqrt{R_{11}^2 + R_{22}^2 + \ldots + R_{nn}^2} \tag{54}$$

6.5 Comparative study

Many researchers have tried to identify structural damage by the knowledge of the reduction level of the natural frequencies of the damaged structure. The advantage of this procedure respect others that uses different DSCs lies in its facility to measure and its global character, i.e. its theoretical capacity to detect local and global damage as well. However, its application to real practice presents two main limitations.

The first occurs due to the fact that significative damage can cause small changes on the frequency values and these changes can be overlooked and mixed up with other causes like the instrument precision The other limitation is caused by the uncertainty related to changes of environment or in the structure mass distribution.
An alternative DSC to the frequency is to use the information on changes in the vibration modes when a damage occurs in the structure. The advantage of this procedure lies on the higher capability of the modes to capture local damages than the frequencies. However, this DSC presents some inconveniences. The first, the damage, typically a local phenomenon, may not affect significatively to a mode of a particular order. This can happen in modes of low order, that are common in the free vibration of civil structures, usually of large mass and stiffness. Another inconvenience corresponds that the mode shapes, may be, can be also affected by the environment conditions, traffic loading or inconsistent positions of the measurement sensors. Finally, the number od sensors and their positions can also have importance on the accuracy of the procedure of damage detection.
In relation to the remaining DSCs in the publication [NVH02] a study based on some of the former derivatives of modes of reinforced concrete beams have been carried out. From this study the following conclusions have been drawn.

- The natural frequencies of a reinforced concrete beam are sensitive to damage accumulation, i. e., to the presence of new cracks, but not to the their position. The frequency decrease is monotonic and this property is a good indicator for estimation of damage intensity evolution along time.
- The indexes are less sensitive to damage than the natural frequency but they can give a good indication about the symmetry or antisymmetry of the damage.
- From the evolution of the indexes $COMAC$ it is possible to detect and localize the damage in reinforced concrete beams, but the decrease of these indexes can not permit the evaluation of the damage intensity and its extension.
- When the damage is not local and therefore concentrated at a section, i.e. it is extended to several elements, the decrease of the flexibility as indicator can not permit an easy localization of the crack, but can be valid for its detection
- With the use of the damage indexes it is possible to detect and localize in reinforced concrete beams local damages, non extended cracks, in a mor precise way than with the application of other methods like $COMAC$ and flexiblity. However, it is very difficult, like in other methods, to localize cracks when they are extended. In any case, the crack severity evolution can be tracked by means of the computation of the natural frequencies.

7 Elastic model of the beam with cracks

7.1 Introduction

As it has been already commented three main groups of the dynamic behavior of cracked reinforced concrete beams subjected to free vibrations have reported in the technical literature. In the first group, represented by the works of [LCC04], [Lin04], [SFE02], [CB84] among others, it is assumed the cracks do not modify their position and geometry during the the beam vibrations. This hypothesis means small amplitude vibrations around a static equilibrium position. In the second group of models a bilinear behavior for the cracks is considered. When the vibration tends to close the crack, the damage section behaves as uncracked. By the contrary if the crack increases its opening the corresponding section has a damaged stiffness. This group of models, apparently more elaborated can be more suitable for metallic structures but no for reinforced concrete beams. In fact, in concrete estructures the aggregate, when cracks are closing, prevents their total closure. Finally, in the third group of models, the crack behavior is simulated by the introduction of elastic springs with characteristics varying with time according to beam response in its free vibrations. As it has been shown in the experimentation carried out in [NPM$^+$00] the behavior of reinforced concrete beams with cracks under free vibrations is nonlinear and depends on the amplitude of vibrations. However, the DSCs values are not significatively affected by this fact, except the damping critical ratio. As a consequence, damping proportion is normally considered an unreliable DSC in order to identify locate damage. In addition, recent studies [NWM02] and [NVH02] have shown the importance of the damage level on the reduction of the structural stiffness and also the need to use an adequate model, moment - relative rotation, for sections with cracks.

The theorem of Hu-Washizu (H-W), developed independently in [Hu,55] and [Was82], has been applied in [CB84] in order to derive the Navier Bernoulli (N-B) beam with cracks subjected to free vibrations. The obtained approximated damaged beam equations are dependent on an estimated function called crack function. In this way the presence of a crack in the beam is simulated by a continuous reduction of the stiffness of beam cross-sections, significative important near the crack. This stiffness reduction is dependent on the crack position and its depth. Then, it is possible to model the cracked beam using the FE method and with this model to identify both, crack position and severity, by solving the inverse initial boundary value problem of free vibrations as is reported in [SFE02]. Here, in this paper the former formulation has been extended to cope the situations of several cracks and non symmetric damage, i.e. cracks situated only in one of two free faces, bottom and top faces, of the beam.
The variational equation represented by the theorem of (H-W) is specialized to a straight uncracked beam of Navier-Bernoulli. The following notation for the beam is introduced

1. A cartesian rectangular coordinate system $Oxyz$ is considered.
2. The abscissae axis Ox coincides with the straight beam axis. The axes Oy and Oz are parallel to the principal axes of the beam cross section of the beam.
3. The origin O of coordinate axes is the gravity center of the left end cross section of the beam.
4. The displacement field of the beam is u, v, w.
5. The distributed forces $f_z \neq 0$, parallel to axis Oz, are acting per unit of volume.

and the hypothesis of Navier-Bernoulli are summarized as follows:

1. The displacement field is defined by the relations

$$u = u(x,z,t), \quad v = 0, \quad w = w(x,t), \quad u = -zw' \tag{55}$$

in which h' denoted the first derivative of a generic function h respect to abscissa x and $\dot{h}$ its time derivative.

2. Then the strain field is

$$\varepsilon_{xx} = -z\kappa \quad \text{with} \quad \kappa = \kappa(x,t) \tag{56}$$

with κ the curvature at section x. The remaining strains are

$$\varepsilon_{yy} - \nu\varepsilon_{xx}, \quad \varepsilon_{yy} - \nu\varepsilon_{xx}, \quad \varepsilon_{xy} = \varepsilon_{xy} = \varepsilon_{yz} = 0 \tag{57}$$

3. The stress field is written as

$$\sigma_{xx} = -zm, \quad \sigma_{xz} = \sigma_{xz}(x,z,t) \quad \text{with} \quad m = m(x,t) \tag{58}$$

in which m represents the bending moment at section x divided by the second moment of the section.

4. Finally the velocities field is defined by the equations

$$p_x = 0, \quad p_y = 0, \quad p_z = p(x,t) \tag{59}$$

where the function $p(x,t)$ express the fact that only translational inertial or D'Alambert forces along the axis z are considered. Inertia forces caused by rotation of beam sections are neglected.

If the former fields of the beam variables are introduced in the variational formulation of the H-W theorem the classical equation for the dynamic vibration of a beam is obtained.

$$(EIw'')'' + A\rho\ddot{w} = f(z) \tag{60}$$

with $A = A(x)$ and $I(x)$ the area and second moment of the section x. The elasticity modulus and density of the material are E and ρ respectively. The domain equation (60) together with the corresponding boundary conditions are sufficient to find the dynamic response of the beam.

7.2 Navier-Bernoulli beam with cracks

The former formulation for the uncracked beam can be extended to the case of a beam with only one crack as it is shown in figure 12.

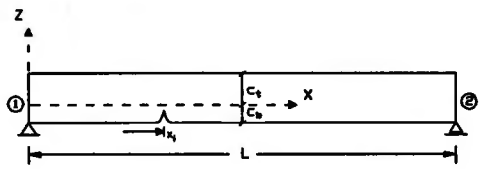

Figure 12: Beam with a crack

It is assumed that the crack presence modifies only the strain and stress fields respect to the fields of the uncracked beam. Moreover, this modification applies only to longitudinal strains and stresses, i.e. to σ_{xx} and to ε_{xx}. Then the existence of the crack does not modify the velocity and displacement fields. Therefore, the following fields are assumed, with $f(x,z)$ a function to be estimated called crack function:

1. Displacement field
$$u = -zw', \quad v = 0, \quad w = w(x,t) \tag{61}$$

2. Strain field
$$\varepsilon_{xx} = [-z + f(x,z)]k(x,t), \quad \varepsilon_{yy} = \varepsilon_{zz} = -\nu\varepsilon_{xx}, \quad \varepsilon_{xy} = \varepsilon_{xz} = \varepsilon_{yz} = 0 \tag{62}$$

3. Stress field
$$\sigma_{xx} = [-z + f(x,z)]m(x,t), \quad \sigma_{xz} = \sigma_{xz}(x,z,t), \quad \sigma_{zz} = \sigma_{xy} = \sigma_{xz} = \sigma_{yz} = 0 \tag{63}$$

4. Velocity field
$$p_x = 0, \quad p_y = 0, \quad p_z = p(x,t) \tag{64}$$

The application of the H-W theorem to this case leads to the following equation of the cracked N-B beam of length L:
$$[E(I - K_{11})Hw'']'' + \rho A\ddot{w} = 0 \quad \text{en} \quad x \in (0,L) \tag{65}$$
that represents the general equation governing the dynamic behavior of N-B beam with one crack subjected to free vibrations. The following notation has been used
$$K_{mn}(x) = \int_{z_b(x)}^{z_t(x)} b(z)z^m f^n(x,z)dz \quad (m,n = 0,1,2,\ldots)$$
with $b(z)$ the width of the constant section at coordinate z. As particular cases, the area is $A = K_{00}$ and the second order moment is $I = K_{20}$. The function $H(x)$ is expressed in terms of the former functions as follows
$$H(x) = \frac{I - K_{11}}{I - 2K_{11} + K_{02}}$$
The boundary conditions are formulated as follows:

- Static or force conditions
$$-M_y + \epsilon(K_{11} - I)EHw'' = 0, \quad Q_z - \epsilon(I - K_{11}E(Hw'')' = 0 \tag{66}$$
with $\epsilon = -1$ if $x = 0$ and $\epsilon = 1$ in the case $x = L$.

- Kinematic or displacement conditions
$$w' = -\overline{\theta}, \quad w = \overline{w} \tag{67}$$

It can be observed that in the case of uncracked beam the crack function $f = f(x, z, t)$ is null and therefore $K_{11} = 0$ and $K_{02} = 0$. Then, the differential domain equation (65) and the boundary conditions, (66) and (67), become to the well known N-B equations.
By inspection of the domain equation (65) and the boundary conditions, (66) and (67) it is realized that the behavior of a beam with a single crack at an specified section is similar to the behavior of an uncracked beam of longitudinally variable section. The variation law of the equivalent second order moment, $I_{eq}(x)$, is given by the following expression:

$$I_{eq}(x) = (I - K_{11})H \quad \text{with} \quad H = \frac{I - K_{11}}{I - 2K_{11} + K_{02}} \tag{68}$$

From the former discussion it is obvious the importance of a suitable selection of the crack function in order to model adequately the dynamic response of a beam with crack. In the next section this topic will be discussed

7.3 Crack Function

The case of a beam of symmetric constant cross-section with two symmetric cracks, one at each face, bottom and top, of the beam with equal depth has been studied by [CB84]. The crack function obtained by physical reasoning was an exponential function. Here this result will be extended to cope other crack pattern. First, the presence of a single crack appearing at one of the two faces of the beam is modelled. Then, the existence of several cracks, each of different depth, will be considered. In all cases it will be assumed constant cross-section of the beam, although nonsymmetric. In the figure (13) the notation and the system of coordinate axis used in this case are shown.

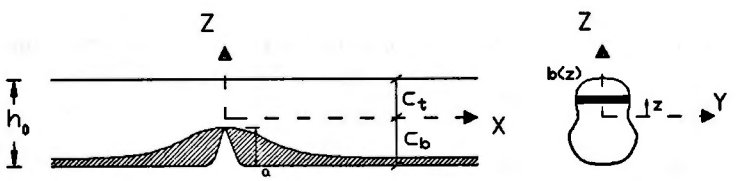

Figure 13: Crack function. Beam with constant nonsymmetric cross-section

The data used to define the model when the crack is situated at bottom face are crack position x_i and depth a_i. The gravity center of the constant cross-section is defined by the distances, c_t and c_b, to the two faces, top and bottom, of the beam respectively. Then, the beam height is h_0 such that $h_0 = c_t + c_b$. The width variation of the section is given by the function $b(z)$ of the coordinate z. In the following two dimensionless variables are introduced: *the ratio* μ between the second order moments of the uncracked section and the cracked section and *the relative abscissa* u. Both are defined by the expressions:

$$\mu = \frac{I}{I_r} = \frac{\int_{-c_b}^{c_t} b(z)z^2 dz}{\int_{-c_b+a_i}^{c_t} b(z)(z - z_g)^2 dz}, \quad \mu = \alpha \frac{|x - x_i|}{h_0} \tag{69}$$

with z_{gi} the gravity center of the cracked section, that can be found by the formulae

$$z_g = \frac{\int_{-c_b+a_i}^{c_t} b(z)z dz}{\int_{-c_b+a_i}^{c_t} b(z) dz}$$

and α is a parameter to be estimated by experimentation. The value $0.667 \times 2 = 1,334$ have been suggested in [CB84].
Using a similar line of work as in [CB84] the variation of the effective resistant cross-section in terms of the dimensionless abscissa u can be found as follows:

- At cracked section $x = x_i$ there exist two limits, a bottom and a top limits, for the effective section, given by the expressions

$$z_t^0 = c_t, \quad z_b^0 = a - c_b$$

- At a far away section from the crack, in theory at $x = \infty$, the effective section is the whole uncracked section, i.e.

$$z_t^\infty = c_t, \quad z_b^\infty = -c_b$$

- Assuming an exponential variation of the limits of the effective section, the limits for a generic section of abscissa x are:

$$z_t = z_t(x) = c_t, \quad z_b = z_b(x) = ae^{-u} - c_b$$

The extreme longitudinal stresses, σ_{xx}, vary along the beam according to the following considerations:

- At section $x = x_i$ the stresses are

$$\sigma_{xt}^0 = -\mu(c_t - z_g)m, \quad \sigma_{xb}^0 = -\mu(a - c_b - z_g)m$$

- At a far away section from the crack

$$\sigma_{xt}^\infty = c_t m, \quad \sigma_{xb}^\infty = c_b m$$

- At a generic section defined by the abscissa x

$$\sigma_{xt} = \sigma_{xt}(x) = (\sigma_{xt}^0 - \sigma_{xt}^\infty)e^{-u} + \sigma_{xt}^\infty, \quad \sigma_{xb} = \sigma_{xb}(x) = (\sigma_{xb}^0 - \sigma_{xb}^\infty)e^{-u} + \sigma_{xb}^\infty$$

The stress at a fiber z of section x can be found by interpolation from the former values:

$$\sigma_{xx}(x, z) = [\sigma_{xb}(x)(1 - \eta) + \sigma_{xt}(x)\eta]H[z - z_b(x)]m \tag{70}$$

with $H[z - z_b(x)]$ the Heaviside function and η an dimensionless function of the coordinate z, with values in $0, 1)$. They can be defined according to the expressions:

$$\eta = \frac{z - z_b(x)}{z_t(x) - z_b(x)} \quad \text{and} \quad H[z - z_b(x)] = 1 \text{ for } z \geq z_b(x) \quad H[z - z_b(x)] = 0 \text{ for } z < z_b(x)$$

and the value of the crack function $f(x, z)$ is, according to its definition:

$$f(x, z) = -z + \sigma_{xs}(x, z) \tag{71}$$

Once determinate the crack function $f(x, z)$ thee characteristics of the equivalent section can be obtained by computation of the following integrals over the whole section of the beam (numerical evaluation is advisable):

$$K_{mn}(x) = \int_{z_b(x)}^{z_t(x)} b(z)z^m f^n(x, z)dz$$

in which $A = K_{00}$ and $I = K_{20}$. The function $H(x)$ is

$$H(x) = \frac{I - K_{11}}{I - 2K_{11} + K_{02}}$$

The equivalent second moment I_{eq} of the section x is

$$I_{eq}(x) = (I - K_{11})H \tag{72}$$

A possible simplification is to introduce a linear expansion in e^{-u}. Then is is obtained:

$$f(x, z) = \overline{f}(z)e^{-u} \tag{73}$$

where

$$\overline{f}(z) = (h_0 - c_b)\overline{a} + \mu a(\frac{1}{2} - \overline{c}_i) + \overline{z}(h_0 - a)(1-\mu), \quad \overline{a} = \frac{a}{h_0}, \quad \overline{c}_i = \frac{c_b}{h_0}, \overline{z} = \frac{z}{h_0}$$

and the former integrals are now

$$K_{mn}(x) = \overline{K}_{mn} e^{-nu} \tag{74}$$

with the following functions of x:

$$\overline{K}_{mn} = \int_{z_b(x)}^{z_t(x)} b(z) z^m \overline{f}^n(z) dz$$

If there exist B cracks, $i = 1, 2, \ldots, B$, situated along the bottom face of the beam, then the effective section of the beam at abscissa x is the one produced by the crack function $f_{i_{max}}(x, z)$, corresponding to the crack $i_{max} = i_{max}(x)$. This crack causes the maximum reduction of the actual section at x of the beam i. e. it satisfies the condition

$$z_{i_{max}} = \max_{i=1,2,\ldots,B} [z_b(x)] \tag{75}$$

The characteristics of the section x are computed by the formula

$$K_{mn}(x) = \int_{z_{i_{max}}(x)}^{z_t(x)} b(z) z^m f^n_{z_{i_{max}}}(x, z) dz$$

and the second moment for the section x is given by the expression (72).
If there exist B cracks, $i = 1, 2, \ldots, B$, situated along the bottom face of the beam and T cracks, $j = 1, 2, \ldots, T$, along the top face, then for each section x two cracks are identified, bottom crack $i_max = i_{max}(x)$ and top crack $j_min = j_{min}(x)$, that are the ones producing the limits of the effective section, i. e. they satisfy the following conditions:

$$z_{i_{max}} = \max_{i=1,2,\ldots,B} [z_b(x)], \quad z_{j_{min}} = \min_{j=1,2,\ldots,T} [z_t(x)] \tag{76}$$

These two limiting crack are used in order to obtain the equivalent second order moment at section x by applying the formula (72), modified according to the following expressions

$$K_{mn}(x) = \int_{z_{i_{max}(x)}}^{0} b(z) z^m f^n_{i_{max}}(x, z) dz + \int_{0}^{z_{j_{min}}(x)} b(z) z^m f^n_{j_{min}}(x, z) dz \tag{77}$$

or to the equivalent formulae

$$K_{mn}(x) = \int_{z_{i_{max}(x)}}^{0} b(z) z^m \overline{f}^n_{i_{max}}(z) dz e^{-nu_{i_{max}}} + \int_{0}^{z_{j_{min}}(x)} b(z) z^m \overline{f}^n_{j_{min}}(x, z) dz e^{-nu_{j_{min}}} \tag{78}$$

in which it has been used the obvious extended notation.

7.4 Equation of the dynamic equilibrium of the structure

Using the former results it is possible to find at each point s of the beam the effective section. In a general case, if a FE method is used to model a beam with cracks, then for each element joining the nodes 1 and 2, and with a length a, the stiffness matrix $\mathbf{k}$ and the mass matrix $\mathbf{m}$ can be computed as by means of the standard formulae:

$$\mathbf{k} = [k_{ij}] \quad \text{with} \quad k_{ij} = a \int_0^1 N_i''(\xi) EI(x) N_j'' d\xi \quad i, j = 1, 2, 3, 4 \tag{79}$$

$$\mathbf{m} = [m_{ij}] \quad \text{with} \quad m_{ij} = a \int_0^1 N_i(\xi) \overline{m} N_j d\xi \quad i, j = 1, 2, 3, 4 \tag{80}$$

with x the abscissa measured from the node 1 of the element, $\xi = \frac{x}{L}$ a dimensionless variable with values in the interval $(0, 1)$. The shape functions are Hermite cubic polynomials. The second order moment

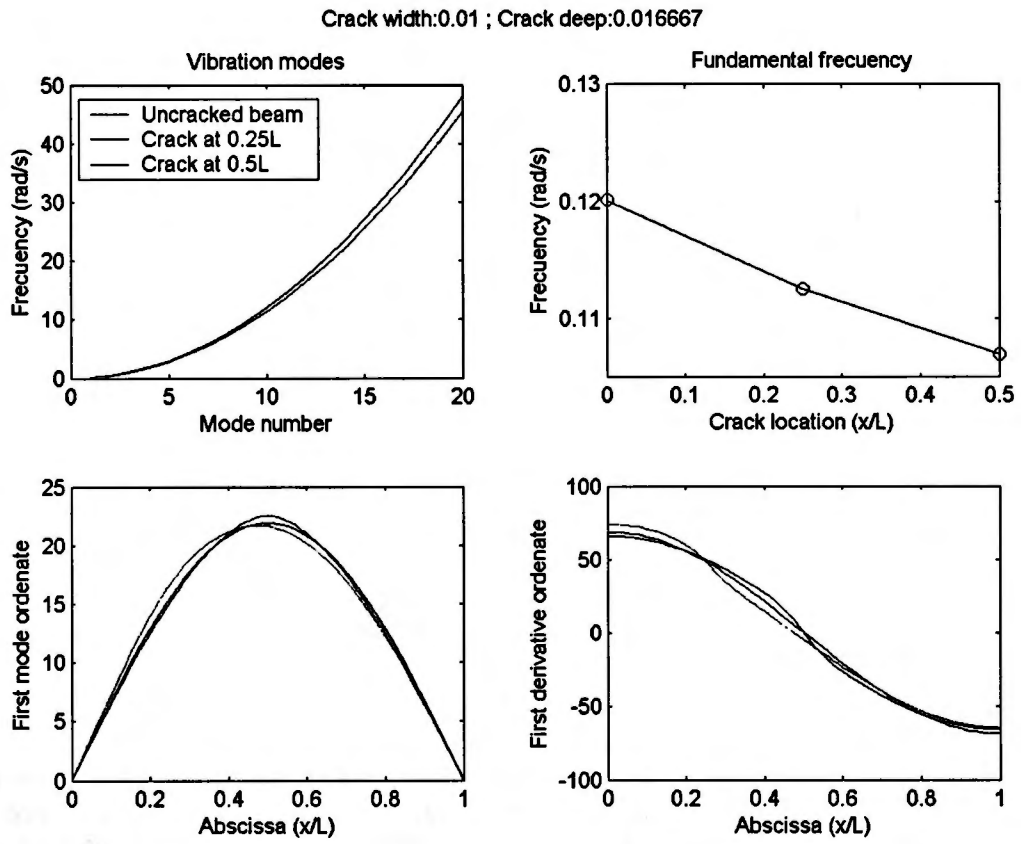

Figure 14: Example. Comparative analysis among cracked and uncracked beams

$I(x)$ varies within the element and it is computed according with the already presented formulae. Finally the variable $\overline{m}$ is the mass per unit of length or intensity of the distributed mass along the whole length of the element.

7.5 Numerical example

In order to illustrate the potentialities of the model, it will be applied to a simple example, defined with the following data expressed in a consistent unit system MKS.
A simple supported beam of span L with rectangular constant section of height $h = \frac{L}{15}$ and width $b = \frac{L}{40}$, i.e. with second order moment $I = \frac{1}{12}bh^3$. The beam material density is $\rho = 2.5$ and its elasticity modulus E. First the analysis is carried out for two crack positions. In the first the crack is situated at section $x = \frac{L}{4}$ with a penetrating depth $a = 0.01667L$ and the second position the crack es at $x = \frac{L}{4}$ with the same depth. In figure (14), composed by four groups of graphs, the values of different DSCs for the uncracked and the two cracked beams are shown. In the first group, the differences obtained for the first twenty natural frequencies are represented. Also in the second group the variation of the value of the first frequency in terms of the crack location is given. Finally, in the two remaining groups of graphs the first mode and its first derivative for the three beams are drawn. As it can be observed the first mode shape is more sensitive to the crack position than the value of first natural frequency. First derivative of the mode is even more sensitive than the model shape itself respect to crack position. The damage severity is described by the depth of the crack penetration. Finally figure (15) represents the modification of the first derivative of the first mode of the cracked beam at $x = \frac{L}{4}$ modifies its severity, from a zero values (no cracks) up to $0,6h$, i.e. a sixty per cent of the beam height.

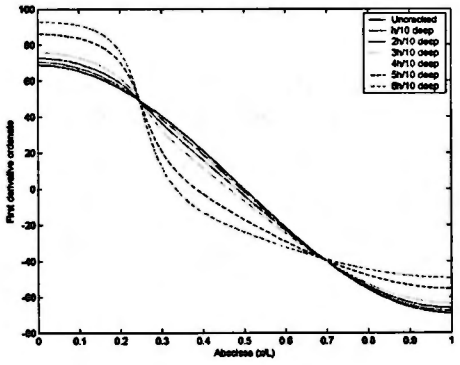

Figure 15: Example. Crack at $x = \frac{L}{4}$. Sensitivity of the first derivative of the first mode respect to crack depth

8 Concluding remarks

In the maintenance of structures damage detection represents a very important task. Despite the intensive research and contributions developed during the last decades there no is a single and universal methodology to detect and locate potential damages in structures. Restricting the damage to cracks, the detection methods should considered the possibility to perform tests under controlled environment, like, laboratories or to be taken place in different circumstances as usually occur in already built structures. Also structures made with homogeneous materials as metallic materials and other built with more complex materials as reinforced concrete demand different methodology. In general, methods based on dynamic tests seem to be very common and efficient tools to identify and control structural damage. The design of a suitable dynamic excitation, that can be dependent on the type of damage to be investigated, may facilitate the detection of this damage and in some cases avoid the step concerned with the solution of the difficult inverse or identification problem of the damage.

9 Acknowledgements

The authors wish to express their acknowledgments to the Spanish Ministry of Science and Technology for its partial financial support of this publication under the research project DPI2002-04412-C03-03.

References

[ASM04] Ananda Rao, M., Srinivas, J., and Murthy, B. S. N. Damage detection in vibrating bodies using genetic algorithms. *Computers and Structures*, 82:963–968, 2004.

[BW96] Bäumgartner, W. and Waubke, H. Traffic load assessment of bridges by permanent stress measurement. In *Proc. Third Conference on Bridge Management*, April 1996.

[CB84] Christides, S. and Barr, A. D. S. One dimensional theory of cracked bernoulli-euler beams. *International Journal of Mechanical Science*, 26:639–648, 1984.

[DT04] Dutta, A. and Talukdar, S. Damage detection in bridges using accurate modal parameters. *Finite Elements in Analysis and Design*, 40:287–304, 2004.

[Fed97] Federal Highway Administration. The status of the nations's highway bridges. Report to the United States Congress 13, University of California, Berkeley. Earthquake Engineering Research Center, 1997.

[HS97] Hjelsmstad, K. D. and Shin, S. Damage detection and assessment of structures from static response. *Journal of Engineering Mechanics*, 123(6):568–576, 1997.

[Hu,55] Hu, H. Ch. On some variational principles in the theory of elasticity and plasticity. *Scientia Sinica*, 4:33–55, 1955.

[KH03] Kao, C. Y. and Hung, S. L. Detection of structural damage via free vibration responses generated by approximating artificial networks. *Computers and Structures*, 81:2631–2644, 2003.

[LCC04] Lee, J. S., Choi, I. Y., and Cho, H. N. Modelling and detection of damage using smeared crack model. *Engineering Structures*, 26(2):267–278, 2004.

[Lin04] Lin, H. P. Direct and inverse methods on free vibration analysis of simply supported beams with a crack. *Engineering Structures*, 26(4):427–436, 2004.

[LL59] Landau, L.D. and Lifshitz, E.M. *Theory of Elasticity*, volume 7 of *Course of Theoretical Physics*. Pergamon Press, New York, 1959.

[MFH+90] Mirza M. S:, Fedjani, O., Hadj-Arab, A., Joudar, K., and Khaled, A. An experimental study of static and dynamic response of prestressed concrete box girder bridges. *Canadian Journal of Civil Engineering*, 17(3):481–493, 1990.

[NPM+00] Ndambi, J. M., Peeters, B., Maeck, J., De Visscher, J., Wahab, M: A., Vantomme, J., De Roeck, G., and De Wilde, W. P. Comparison of techniques for modal analysis of concrete structures. *Engineering Structures*, 22(9):1159–1166, 2000.

[NVH02] Ndambi, J. M. , Vantomme, J., and Harri, K. Damage assessment in reinforced concrete beams using eigenfrequencies and mode shape derivatives. *Engineering Structures*, 24(4):501–515, 2002.

[NWM02] Neild, S. A., Williams, M. S., and McFadden, P. D. Nonlinear behavior of reinforced concrete beams under low amplitude cyclic and vibration loads. *Engineering Structures*, 24(6):707–718, 2002.

[PBS91] Pandey, A. K., Biswas, M., and Samman, M. M. Damage detection from changes in curvature mode shape. *Journal of Sound and Vibration*, 145(2):321–332, 1991.

[PDPS95] Peeters, B., De Roeck, G., Pollet, L., and Schueremans, L. Stochastic subspace techniques applied to parameter identification of civil engineering structures. In *Proc. of New Advances in Modal Synthesis of Large Structures: Nonlinear, Damped and Nondeterministic Cases*, pages 151–162, October 1995.

[Rab01] Rabinovotch, O. and Frostig, Y. Nonlinear high-order analysis of cracked RC beams strengthened with FRP strips. *ASCE. Journal of Structural Engineeering*, 127(4):381–389, 2001.

[RD00] Royer, D. and Dieulesaint, E. *Elastic Waves in solids. Vol I and II.* Springer Verlag, Berlin-Heidelberg, 2000.

[Sal97] Salawu, O. S. Detection of structural damage through changes in frequency: a review. *Engineering Structures*, 19(9):718–723, 1997.

[SFE02] Sinha, J. K., Friswell, M. I., and Edwards, S. Simplified models for the location of cracks in beam structures using measured vibration data. *Journal of Sound and Vibration*, 251(1):13–38, 2002.

[SM02] Samartín, A. and Moreno, C. Application of the dynamic models to the detection of imperfections in plate structures. In *Proceedings of The Eight International Conference on Computational Structures Technology*, pages 1–19. Prague, Czech Republic, 2002.

[SS91] Sanayei, M. and Scampoli, S. F. Structural element stiffness identification from static test data. *Journal of Engineering Mechanics*, 117(5):1021–1036, 1991.

[Was82] Washizu K. *Variational Methods in Elasticity and Plasticity.* Pergarmon Press, Oxford. England, 1982.

[WHFY01] Wang, X., Hu, N., Fukunaga, H., and Yao, Z. H. Structural damage identification using static test data and changes in frequencies. *Engineering Structures*, 23(6):610–621, 2001.

[Yue85] Yuen, M. N. F. A numerical study of the eigenparameters of a damaged cantilever. *Journal of Sound and Vibration*, 103(3):301–310, 1985.